

Piezoelectric actuator technology

Craig D. Near

Materials Systems Inc.
521 Great Road, Littleton, MA 01460

ABSTRACT

Piezoelectric actuator technology is reviewed, and the performance of current state-of-the-art piezoelectric actuator devices estimated. Comparisons between actuator configurations show a wide range of available force and displacement performance. General design guidelines for the selection and use of piezoelectric actuators for active vibration and control applications are given. Examples of state-of-the-art actuator devices are given for each actuator case.

Keywords: piezoelectric actuator, Bimorph, Rainbow, patch actuator, tubular actuator, multilayer actuator, PZT.

1. INTRODUCTION

Piezoelectric actuator devices offer a number of benefits for applications in active vibration control systems. Their high stiffness results in high actuator authority. The actuators are easily controlled and modeled due to their near linear response with applied voltage. Many actuator configurations are reliable and have low cost, including Bimorphs®, Rainbows®, and patches. Tubular actuators offer many advantages in linear positioning and pointing applications. Newer high power multilayer actuators are being developed and optimized for high stiffness, strain, and efficiency. Current piezoelectric actuators offer either low displacement with high force (monolithic or multilayer ceramic actuators) or high displacement with low force (piezoelectric benders).

Piezoelectric actuators have been demonstrated in many active noise and vibration control applications. These applications include: active control of helicopter rotor vanes and airfoil contours, active vibration damping (struts and engine mounts), noise suppression (interior and engine noises), acoustic camouflage, actuated structures, precision pointing (optical and radio frequency payloads), reconfigurable surfaces (flutter suppression), and structural health monitoring. These applications require a wide range of actuator displacement and authority. A high power actuator requirement, given by Straub for a servoflap for helicopter rotors, required 1.37mm displacement, 6160N force, at 19.3Hz, or 510 watts mechanical power.¹ Similar requirements were given by Giurgiutiu for individual blade control (IBC) for vibration reduction in helicopter rotors.² This system required ± 1 mm displacement, 1300N force, at 30Hz, or 245 watts mechanical power. A lower power helicopter application, given by Samak for a helicopter rotor flaperon, required 0.25mm displacement, 180N force, at 40Hz, or 6 watts mechanical power.³ Many positioning or pointing applications demand much less authority. For example, optical aberration correction using a deformable mirror would require 5 μ m displacement, 0.002N load, at 1kHz, or 30 μ W mechanical power.

The wide range of actuation force, displacement, and authority or power specifications for these active control systems require the proper selection and implementation of appropriate piezoelectric actuator configuration. This paper describes the operational ranges for each major type of piezoelectric actuator. Examples of current state-of-the-art actuators are given to aid comparison and selection. In addition, the behavior of PZT actuator materials are discussed to help selection for a given application. Suggested selection criteria, issues, and approaches are given.

2. DEFINITIONS AND UNITS

Table 1 lists the definitions and units for all parameters used in describing the piezoelectric actuator devices.

Table 1. Definitions and Units

Variable	Definition	Unit
K_{33}^T	PZT dielectric constant	
ϵ_0	permittivity of free space	8.854×10^{-12} farad/meter
$\tan\delta$	PZT dielectric loss	
Q_M	PZT mechanical Q	
k_{33}	PZT longitudinal coupling coefficient	
k_{31}	PZT transverse coupling coefficient	
d_{33}	PZT longitudinal piezoelectric charge constant	meter / volt
d_{31}	PZT transverse piezoelectric charge constant	meter / volt
g_{33}	PZT longitudinal piezoelectric voltage constant	volt * meter / newton
g_{31}	PZT transverse piezoelectric voltage constant	volt * meter / newton
Y_{33}^E	PZT longitudinal, short circuit Young's modulus	newton / meter ²
Y_{11}^E	PZT transverse, short circuit Young's modulus	newton / meter ²
L	actuator length	meter
w	actuator width	meter
t	actuator thickness	meter
h	actuator height	meter
t_c	PZT ceramic layer thickness	meter
τ	bimorph vane thickness	meter
k_b	maximum bending coupling coefficient	
f	frequency	hertz
C	actuator capacitance	farad
I	actuator drive current	ampere
V	actuator drive voltage (peak to peak)	volt
E_E	electric field (peak to peak)	volt / meter
ΔL	actuator peak displacement	meter
F_b	actuator block force	newton
E	maximum actuator energy output	joule
P_E	actuator reactive electrical input power	watt
P_{DE}	actuator dissipated electrical power	watt
P_M	maximum actuator mechanical output power	watt
P_{DM}	actuator dissipated mechanical power	watt
ΔP	maximum actuator efficiency	%
Q_T	actuator transducer mechanical Q	

5. BIMORPH[®] ACTUATORS

The bimorph is a common configuration for the actuation of relatively large bending displacements with low load. The first reported bimorph device was a bilaminate of quartz by J. Curie.⁴ Bimorphs can be configured either as a rectangular or a circular bender. The rectangular bimorph may be mounted either as a cantilever or a simple beam. Bimorphs may be configured either as a series or parallel type depending on the direction of polarization and operational fields.

Expressions for force and deflection of the various bimorph configurations have been approximated by C.P. Germano.^{5,6,7} Table 2 below shows the expressions for a rectangular series bimorph. Though the displacement for a parallel bimorph is twice that for a series bimorph, its maximum mechanical power output is equivalent. Germano's analysis is not rigorous, but usually suffices for design purposes. The expressions apply for low frequencies, appreciably below resonance, which is usually suitable for "smart" systems applications. Also, all expressions assume ideal bonding of the two ceramic layers to the internal metal vane, internal metal vane layer thickness of τ , and ideal mounting of the bender to the support structure. Since the electromechanical coupling k_b for the bimorph is dependent on the bimorph geometry, the maximum coupling is given in Table 2 below.

Table 2. Expressions for Rectangular Series Bimorph Actuation⁵

Parameter	Cantilever	Simple Beam
Capacitance (C)	$K_{33}^T \epsilon_0 L w / (2 t_c)$	$K_{33}^T \epsilon_0 L w / (2 t_c)$
Current (I)	$2\pi f C V (1 + \tan \delta)$	$2\pi f C V (1 + \tan \delta)$
Electrical Power (Reactive) (P_E)	$2\pi f C V^2 (1 + \tan \delta)$	$2\pi f C V^2 (1 + \tan \delta)$
Maximum Coupling (k_b)	$0.75 k_{31}$	$0.75 k_{31}$
Deflection (ΔL)	$1.5 g_{31} (L/wt) C V (1 - (\tau^2/t^2))$	$0.375 g_{31} (L/wt) C V (1 - (\tau^2/t^2))$
Blocked Force (F_b)	$0.375 g_{31} Y_{11}^E t^2 C V (1 - (\tau^2/t^2)) / L^2$	$0.09375 g_{31} Y_{11}^E t^2 C V (1 - (\tau^2/t^2)) / L^2$
Max. Mechanical Power (P_M)	$0.28125\pi f k_{31}^2 C V^2 t (1 - (\tau^2/t^2))^2 / t_c$	$0.0175\pi f k_{31}^2 C V^2 t (1 - (\tau^2/t^2))^2 / t_c$

Typical performance ranges for bimorph actuators are displacements of $<500\mu\text{m}$, forces of $<2.5\text{N}$, frequencies of $<10\text{kHz}$, and temperatures of $<75^\circ\text{C}$. An increase in force to 90N may be achieved at the expense of displacement and reliability by using a co-fired bimorph device. An example of current state-of-the-art series bimorph actuator would have dimensions of approximately 75mm length, 17.5mm width, 0.19mm ceramic thickness, and 0.05mm vane thickness. For a DOD-Type VI (PZT-5H) material, the dielectric constant K_{33}^T is 3400, the piezoelectric d_{31} constant is $275 \times 10^{-12}\text{m/V}$, the piezoelectric coupling k_{31} is 0.39, and the Young's modulus Y_{11}^E is $6.2 \times 10^{10}\text{N/m}^2$. With a maximum recommended field of 0.4MV/m (or 150V), the capacitance would be approximately 104nF , the drive current would be 0.1f mA , the drive power would be 15f mW , the peak displacement would be approximately $2130\mu\text{m}$, the block force would be approximately 0.189N , and the maximum mechanical power would be approximately 1.27f mW , where f is the operational frequency.

4. RAINBOW[®] ACTUATOR

The Rainbow[®] device and the newly developed Cerambow[®] have shown displacement and load carrying capability comparable to or slightly superior to those for the bimorph actuator. Typical performance ranges for the Rainbow actuator are displacements of $<1000\mu\text{m}$, forces of $<500\text{N}$, frequencies of $<10\text{kHz}$, and temperatures of $<100^\circ\text{C}$. The Rainbow actuators are designed to be utilized for point loading. As such, the highly displacive Rainbow configurations tend to be limited by material mechanical reliability.

Equations expressing the actuation of Rainbow actuators have not been developed to date. However, an example of measured performance of current state-of-the-art Rainbow actuators can demonstrate their capability. The example is for 50mm diameter, 0.76mm thick Rainbow made with a DOD-Type VI (C3900) material, which has a dielectric constant K_{33}^T of 3900, a piezoelectric d_{31} constant of 294×10^{-12} m/V, a piezoelectric coupling k_{31} of 0.40, and the Young's modulus Y_{11}^E of 6.9×10^{10} N/m². With a maximum recommended field of 0.5MV/m (or 175V), the capacitance would be approximately 178nF, the drive current would be 0.2f mA, the drive power would be 35f mW, the peak displacement was measured as approximately 90μm, the block force was measured as approximately 7.1N, and the maximum mechanical power would be approximately 2.0f mW.¹⁰

5. PATCH ACTUATOR

Thin piezoelectric sheets or patches have been used for many surface mount and embedded actuation applications in both beams and plates. These sheets utilize the high length-to-thickness ratio amplification of the displacement. Sheets may be composed of one or more layers. Multilayer sheets allow for the independent tailoring of the force output versus the voltage-current requirement.

The expressions of the performance of the patch actuator are given in Table 3. The expressions assume operation well below resonance, such that the mechanical Q is approximately unity. For the typical case where the patch length is more than four times either the width or thickness, the patch electromechanical coupling is given by k_{31} , as shown below in Table 3.

Table 3. Patch Actuation Parameters

Parameter	Expression
Capacitance (C)	$K_{33}^T \epsilon_o L w / t$
Current (I)	$2 \pi f C V (1 + \tan \delta)$
Electrical Power (Reactive) (P_E)	$2 \pi f C V^2 (1 + \tan \delta)$
Coupling (k_{31}^2)	$d_{31}^2 Y_{11}^E / (K_{33}^T \epsilon_o)$
Deflection (ΔL)	$d_{31} V L / t$
Blocked Force (F_b)	$d_{31} V Y_{11}^E w$
Max. Mechanical Power (P_M)	$\pi f k_{31}^2 V^2 C$

Typical performance ranges for embedded patch actuators are displacements of 1 to 5μm, forces of 10 to 100N, frequencies of <20kHz, and temperatures of <175°C. In surface mount applications, the displacements may be larger due to the induced bending motion, at the expense of load and mechanical power, similar to the bimorph case. In addition, the load transfer in surface mount applications is highly dependent on the adhesive used.¹¹ Also, the operational temperature is usually limited by the adhesives used in surface mounting application or by the composite used in an embedded application. As such, mechanical power or authority of the surface mount patch actuator is typically 1000 times lower than that of a multilayer d_{33} actuator.

An example of current state-of-the-art embedded patch actuator would have dimensions of approximately 75mm length, 17.5mm width, and 0.125mm thickness. For a DOD-Type VI (PZT-5H) material, the dielectric constant K_{33}^T is 3400, the piezoelectric d_{31} constant is 275×10^{-12} m/V, the piezoelectric coupling k_{31} is 0.39, and the Young's modulus Y_{11}^E is 6.2×10^{10} N/m². With a maximum recommended field of 0.4MV/m (or 50V), the capacitance would be approximately 316nF, the drive current would be 0.1f mA, the drive power would be 5.0f mW, the peak displacement would be approximately 8.25μm, the block force would be approximately 15N, and the maximum mechanical power would be approximately 0.38f mW, where f is the operational frequency.

6. TUBULAR ACTUATOR

Piezoelectric tubular actuators have been used as linear actuators and positions in many applications which require low voltage, moderate displacements, and low forces. These actuators are typically configured as long, thin walled tubes, with electrodes on the inside diameter (ID) and outside diameter (OD), in order to take advantage of the high length-to-wall thickness ratio amplification of the displacement. Tubes can be manufactured with a wrap around electrode, where the inside electrode is wrapped around one end of the tube, so that both electrical connections may be made on the outside. This configuration is particularly useful if the tubular actuator requires mounting on a rod. Also, tubes can be manufactured with striped electrodes, so that segments can be individually actuated to produce a tilt motion on a mounted device such as a mirror.

The expressions of the performance of the tubular actuator are given in Table 4. Again, the equations assume operation well below resonance, such that the mechanical Q is approximately unity. For the typical case where the tube length is more than four times the outside diameter and the outside diameter is more than four times the wall thickness, the tube electromechanical coupling is given by k_{31} , as shown below in Table 4.

Table 4. Tubular Actuation Parameters

Parameter	Expression
Capacitance (C)	$2 \pi K_{33}^T \epsilon_0 L / \ln(OD / ID)$
Current (I)	$2 \pi f C V (1 + \tan \delta)$
Electrical Power (Reactive) (P_E)	$2 \pi f C V^2 (1 + \tan \delta)$
Coupling (k_{31}^2)	$d_{31}^2 Y_{11}^E / (K_{33}^T \epsilon_0)$
Deflection (ΔL)	$2 d_{31} V L / (OD - ID)$
Blocked Force (F_b)	$2 d_{31} V Y_{11}^E ((0.25 \pi OD^2) - (0.25 \pi ID^2)) / (OD - ID)$
Max. Mechanical Power (P_M)	$4 \pi f k_{31}^2 K_{33}^T \epsilon_0 V^2 L ((0.25 \pi OD^2) - (0.25 \pi ID^2)) / (OD - ID)^2$

Typical performance ranges for a tubular actuator are displacements of 1 to 10 μm , forces of 10 to 1000N, frequencies of <50kHz, and temperatures of <175°C. An example of current state-of-the-art tubular actuator would have dimensions of approximately 50mm length, 5mm OD, and 0.5mm wall thickness. For a DOD-Type VI (PZT-5H) material, the dielectric constant K_{33}^T is 3400, the piezoelectric d_{31} constant is $275 \times 10^{-12} \text{m/V}$, the piezoelectric coupling k_{31} is 0.39, and the Young's modulus Y_{11}^E is $6.2 \times 10^{10} \text{N/m}^2$. With a maximum recommended field of 0.4MV/m (or 200V), the capacitance would be approximately 42nF, the drive current would be 0.05f mA, the drive power would be 11f mW, the peak displacement would be approximately 12.3 μm , the block force would be approximately 33.5N, and the maximum mechanical power would be approximately 1.29f mW.

7. MULTILAYER ACTUATOR

At present, the highest mechanical work density obtained from a piezoelectric device has been achieved with monolithic multilayer d_{33} actuators.¹² The total strain capability for d_{33} actuators produced from "hard" PZT, "soft" PZT, and electrostrictive materials is approximately 0.1%.¹³ "Hard" PZT monolithic actuators have been shown to have a load carrying capability of ~100 MPa.¹⁴

The expressions of the performance of the multilayer d_{33} actuator, with n number of layers, are given in Table 5. The equations assume operation well below resonance, such that the mechanical Q is approximately unity.

Table 5. Multilayer d_{33} Actuation Parameters

Parameter	Expression
Capacitance (C)	$n K_{33}^T \epsilon_0 L w / t$
Current (I)	$2 \pi f C V (1 + \tan \delta)$
Electrical Power (Reactive) (P_E)	$2 \pi f C V^2 (1 + \tan \delta)$
Coupling (k_{33}^2)	$d_{33}^2 Y_{33}^E / (K_{33}^T \epsilon_0)$
Deflection (ΔL)	$n d_{33} V$
Blocked Force (F_b)	$n d_{33} V Y_{33}^E L w / h$
Max. Mechanical Power (P_M)	$\pi f k_{33}^2 V^2 C$

Typical performance ranges for a multilayer d_{33} actuator are displacements of 1 to 25 μm , forces of <35,000N, frequencies of <50kHz, and temperatures of <175°C. An example of current state-of-the-art multilayer d_{33} actuator would contain approximately 190 layers and would have dimensions of approximately 25mm height, 15mm width, 15mm length, and 0.125mm ceramic layer thickness. For a DOD-Type VI (PZT-5H) material, the dielectric constant K_{33}^T is 3400, the piezoelectric d_{33} constant is $595 \times 10^{-12} \text{m/V}$, the piezoelectric coupling k_{33} is 0.75, and the Young's modulus Y_{33}^E is $4.8 \times 10^{10} \text{N/m}^2$. With a maximum recommended field of 2.0MV/m (or 250V), the capacitance would be approximately 10.3 μF , the drive current would be 16.5f mA, the drive power would be 4.1f watts, the peak displacement would be approximately 28 μm , the block force would be 12,200N, and the maximum mechanical power would be 1.1f watts.

8. MECHANICALLY AMPLIFIED ACTUATORS

Piezoelectric actuators have been restricted to either high force or high displacement regimes. High force multilayer actuators tend to have good efficiency, but low displacement. The major limitation of other piezoelectric actuators has been that their various strain amplification schemes have resulted in a sacrifice of high displacement-force transfer efficiency. In addition, current piezoelectric actuators cannot operate in the moderate displacement, moderate force regime, with high mechanical work output and efficiency. As such, many mechanical amplification devices have been designed to work with the multilayer actuator. These amplification devices trade efficiency, temperature operational range, and frequency operational range, in order to actuate in the moderate displacement, moderate force regime.

Flextensional devices, such as Moonies^{15,16,17} and Oysters,¹⁸ have been used as strain amplification devices for both single and multilayer piezoelectric materials. Typical strain amplification of about 5 times is achieved, with up to a 1000-fold decrease in load carrying capability. Most flextensional systems are limited to operational frequencies up to 1kHz. Flextensional systems also have a limited operational temperature range of up to ~50°C, due to thermal expansion mismatch.

Lever systems have been designed to amplify the displacement of piezoelectric actuators, without much sacrifice in efficiency. Performance of lever systems is limited by lever stiffness, geometric constraints, and thermal expansion mismatch. One example is a lever system used by NEC in a printer head application, which has a strain amplification of 30 times and an electromechanical energy transfer of >50%.¹⁹ Modification to the lever design include parallelogram or truss configurations and inertial recoil or meander-line configurations.^{15,20,21,22}

In another example, a hydraulic or elastomeric mechanical amplifier is used. The elastomeric amplifier has been demonstrated by Martin Marietta in its "Fast Acting Control Thruster" (FACT) to provide an order of magnitude strain amplification over monolithic ceramic actuators.²³ These amplifiers also have limited frequency and temperature operational.

9. ACTUATOR PERFORMANCE COMPARISON

Examples of each piezoelectric actuator type are compared in Table 6. The maximum actuator efficiency as a function of the PZT material and the actuator type is given by:

$$\Delta P = P_M / (P_M + P_E). \quad (1)$$

The displacement and force limit estimates for current piezoelectric actuators are shown in Table 7. These force-displacement operational ranges for the current actuators are compared in Figure 1.

Table 6. Performance Comparison of Current State-of-the-Art Piezoelectric Actuators

Device	C (nF)	I (mA)	P _E (watts)	ΔL (μm)	F _b (N)	P _M (watts)	ΔP (%)
Bimorph	104	0.1f	0.015f	2130	0.19	0.0013f	7.9
Rainbow	178	0.2f	0.035f	90	7.1	0.0020f	5.4
Patch Actuator	316	0.1f	0.005f	8.25	15	0.00038f	7.1
Tubular Actuator	42	0.05f	0.011f	12.3	33.5	0.0013f	10.5
Multilayer Actuator	10,300	16.5f	4.1f	28	12,200	1.1f	21.1

Table 7. Maximum Performance Limits of Current Piezoelectric Actuators

Device	Force (N)	Displacement (μm)	Frequency (kHz)	Temperature (°C)
Bimorph	90	500	1 - 10	75
Rainbow	500	1000	1 - 10	100
Patch Actuator	100	10	20	175
Tubular Actuator	1000	10	50	175
Flextensional Amplifier	800	250	1	50
Lever Amplifier	500	750	0.5 - 1	50
Mechanical Amplifier	2000	400	0.5	50
Multilayer Actuator	35,000	25	50	175

10. SELECTION CRITERIA AND ISSUES

General guidelines can be given for selection of a piezoelectric actuator configuration for an active control system. The actuator configuration must be properly matched to both the mechanical and electrical systems requirements. For operation below resonance, the mechanical system specifications include frequency, temperature, duty cycle, force, displacement, and mechanical compliance of the load. The electrical system requirements include frequency, electrical power, and voltage-current requirement. Other considerations include cost, complexity, weight, space allowances, thermal management, reliability, repeatability, hysteresis, and tensile and compressive strengths.

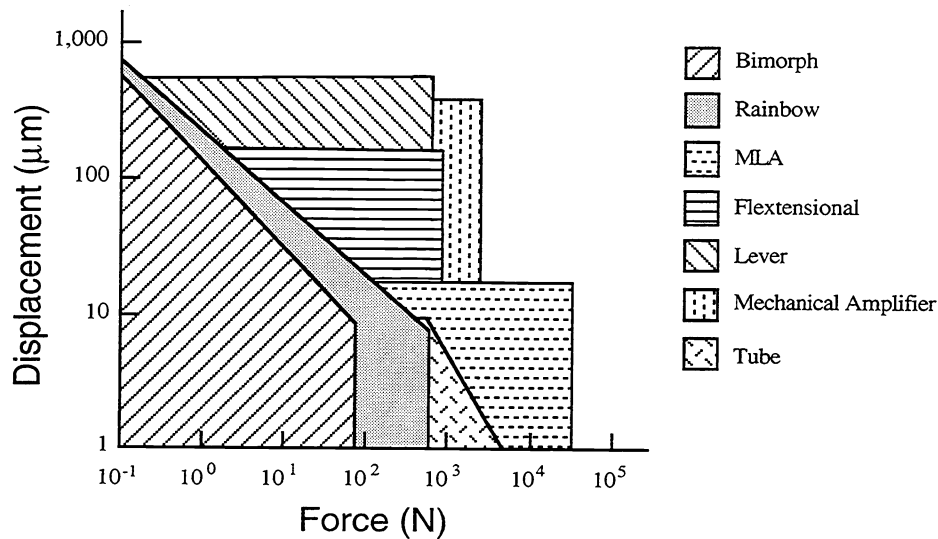


Figure 1. Force-displacement operational ranges for state-of-the-art piezoelectric actuators.

An approach for the selection of an appropriate piezoelectric actuator configuration for a particular application is suggested below.

1. Determine the force and displacement requirements for the active control system.
2. From the above, determine the mechanical power requirements for the system.
3. Select the appropriate piezoelectric actuator by matching the mechanical system requirements to the operational regime of the particular actuator.
4. For an ideally matched actuator, determine the electrical drive power requirements by dividing the mechanical power requirements by the actuator efficiency.
5. Determine the real and imaginary power requirements, by determining the phase between the displacement and load. Select soft PZT material for well-matched, low power systems, and hard PZT for mismatched and/or high power systems.
6. For high power applications, the multilayer actuator may be further tuned by determining the required actuator area from the block force requirements and determining the height from the displacement (strain) requirements. The actuator volume will be determined by the power requirements.
7. For the multilayer actuator applications, downselect to the best operational voltage-current regime to minimize drive electronics cost, by adjusting layer thickness.

11. MATERIAL CONSIDERATIONS

It is convenient to evaluate the properties of piezoelectric actuators at very low drive fields, about 0.01 to 0.001MV/m. However, in operation, the drive level can be as high as 4MV/m.¹³ At high drive levels of about 0.08MV/m for hard PZTs and about 0.02MV/m for soft PZTs, the room temperature properties of piezoelectric ceramic materials change irreversibly due to domain wall motion.²⁴ Domain wall motion significantly increases capacitance, dielectric loss, piezoelectric constant, compliance, and mechanical loss. These high drive properties must be known to properly select and utilize piezoelectric materials and actuator configurations.

PZT property changes have been characterized as a function of temperature, electric field, and stress environmental conditions. Figure 2 shows the change in dielectric constant and piezoelectric d_{33} constant as a function of applied electric field for DOD types II, III, and VI PZT materials.²⁴ Figure 3 shows the change in dielectric constant and dielectric loss as a function of applied electric field at 100Hz for DOD types I, II, and III PZT materials.²⁵ Figure 4 shows the change in mechanical Q and Young's modulus as a function of applied stress for DOD types I and II PZT materials.²⁵ However, the change in properties with respect to changes in two or more environmental conditions have not been characterized.

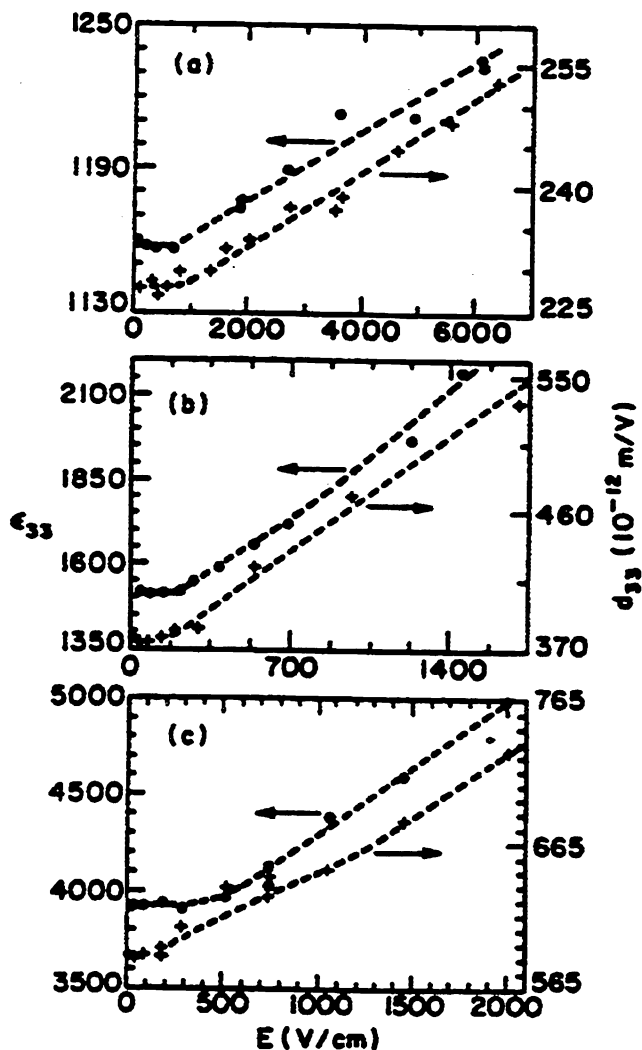


Figure 2. Electric field dependence of the dielectric constant and piezoelectric d_{33} constant, measured at 100 Hz, for: (a) DOD type III (PZT-8), (b) DOD type II (PZT-5A), and (c) DOD type VI (PLZT 7/60/40) materials.²⁴

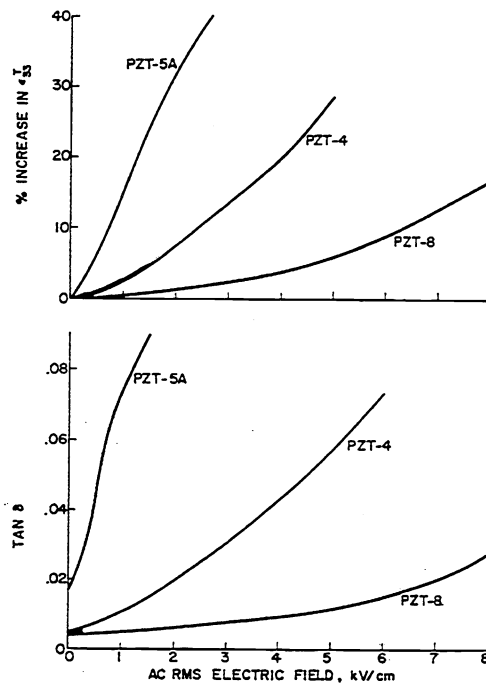


Figure 3. Percent change in dielectric constant and dielectric loss as a function of electric field for: DOD type I (PZT-4), DOD type II (PZT-5), and DOD type III (PZT-8) materials.²⁵

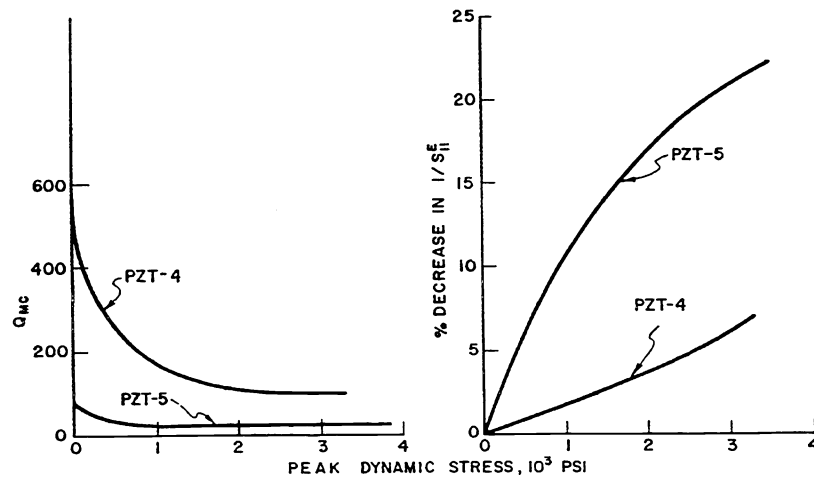


Figure 4. Stress dependence of mechanical Q and Young's modulus ($1/S_{11}^E$) for DOD type I (PZT-4) and DOD type II (PZT-5) materials.²⁵

The high electric field, high stress dielectric and piezoelectric properties should be used to determine the power handling capability of PZT materials for actuator operation under actual usage conditions. The power handling capability per unit volume of a longitudinally driven linear actuator is given by:

$$P_M = \pi f k_{33}^2 E_E^2 K_{33}^T \epsilon_o Q_T, \quad (2)$$

where Q_T is the mechanical quality factor of the actuator transducer assembly, which has been assumed to be near unity for the calculated actuator examples. The dissipated heat power per unit volume of ceramic due to dielectric loss is given by:

$$P_{DE} = \pi f E_E^2 K_{33}^T \epsilon_o \tan \delta. \quad (3)$$

The dissipated heat power per unit volume of ceramic due to mechanical loss in a simple mass loaded transducer is given by:

$$P_{DM} = \pi f E_E^2 k_{33}^2 K_{33}^T \epsilon_o Q_T^2 / Q_M. \quad (4)$$

For the case where the mechanical Q_T of the transducer system is low (<3), the power losses due to the piezoelectric mechanical Q and the piezoelectric phase angle may be neglected.²⁵ Therefore, the material efficiency may given by:

$$\text{efficiency} = P_M / (P_M + P_{DE} + P_{DM}). \quad (5)$$

The actuator material temperature rise due to dissipated power is given by:

$$\Delta T = ((P_{DE} + P_{DM}) - \text{heat removed}) / \text{heat capacity}. \quad (6)$$

As such, the temperature rise is highly affected by thermal management conditions of the system.

The comparison of the power handling capabilities of DOD types I, II, and III PZT materials is shown in Figure 5, where the total heat power ($P_{DE} + P_{DM}$) is plotted as a function of the mechanical power (P_M). Figure 5 uses values calculated from equations 2, 3, and 4, using the high electric field, high stress dielectric and piezoelectric properties given in Figures 3 and 4.²⁵ This figure shows why, for high power applications, hard PZT materials are preferred.

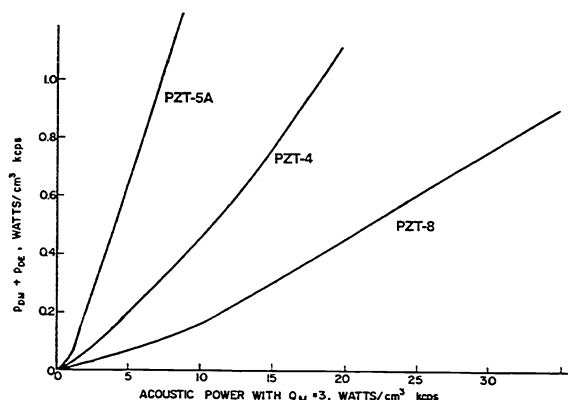


Figure 5. Total dissipated heat power ($P_{DE} + P_{DM}$) as a function of the mechanical (acoustic) power (P_M) for: DOD type I (PZT-4), DOD type II (PZT-5), and DOD type III (PZT-8) materials.²⁵

For bimorph and tubular actuator configurations, the reactive electrical power densities tend to be low. In addition, these devices have high surface-area-to-volume ratio, which improves heat removal. Therefore, soft PZT materials are generally appropriate. However, for multilayer configurations, the reactive electrical power density is high, thereby requiring a low loss hard PZT material. This situation is aggravated by any mismatch in mechanical compliance between the actuator and the load. When the electrical and mechanical reactive powers are mismatched

and the system is run inefficiently, the additional power is dissipated as heat in the ceramic. For this case, hard PZT materials are required to minimize internal heating. An example of this situation is shown in Table 8 for a high power application of a DOD type I (PZT-4S) multilayer d_{33} actuator, with a height of 30mm and outside diameter of 15mm, tested at 200 and 540Hz, under various loads, at 100% duty cycle.¹⁴

Table 8. High Power DOD Type I Multilayer Actuator Performance¹⁴

f (Hz)	E_E (MV/m)	F (N)	P_E (watts)	P_{DE} (watts)	P_M (watts)	P mismatch (watts)	Steady State Temperature (°C)
200	0.7945	3047	48.45	4.76	15.49	32.96	66.9
200	0.8036	5802	45.28	2.28	34.62	10.66	41.0
540	0.8418	2483	154.35	4.89	39.75	114.60	97.0
540	0.8400	6139	146.21	3.60	88.31	57.90	67.6
540	0.8436	9253	153.94	4.92	127.76	26.18	65.3

12. CONCLUSIONS

Piezoelectric actuators are expected to find many uses in active vibration and control systems due to their wide range of force and displacement performance. State-of-the-art actuator types have been described for each actuator case and broad design guidelines for the selection and use of piezoelectric actuators have been given. Precise selection criteria are difficult to establish, since system requirements are broad, and since material and device behavior has not been fully quantified for all operating conditions. Precise material characterization is particularly difficult due to the various possible mechanical compliances and thermal management situations in the various smart system applications.

13. ACKNOWLEDGEMENTS

The author acknowledges the useful discussions and information provided by Mr. Gordon Cooke of EDO Corporation in Salt Lake City, UT, Mr. Andrew Ritter of AVX Corporate Research Center in Myrtle Beach, SC, and Dr. Gerald Stranford of Aura Ceramics Inc. in Minneapolis, MN.

14. REFERENCES

1. F.K. Straub and D. J. Merkley, "Design of Smart Material Actuator for Rotor Control," *Smart Structures and Materials 1995*, Proc. SPIE 2443, pp 89, 1995.
2. V. Giurgiutiu, Z.A. Chaudry, C.A. Rodgers, "Engineering Feasibility of Induced Strain Actuators for Rotor Blade Active Vibration Control," *Smart Structures and Materials 1995*, Proc. SPIE 2443, 1995.
3. D.K. Samak and I. Chopra, "Design of high force, high displacement actuators for helicopter rotors," *SPIE North American Conference on Smart Materials and Structures*, Orlando, FL, Feb. 1994.
4. J. Curie, "Dilatation Electrique Du Quartz," *J. de Physique*, Second Series, vol. VIII, pp 33-55, 1889.
5. C.P. Germano, "Useful Relationships for Ceramic Bender Bimorphs®," TP-223, Morgan Matroc Electro Ceramics Division, Bedford, OH.
6. C.P. Germano, "Useful Relationships for Circular Bender Bimorphs®," TP-230, Morgan Matroc Electro Ceramics Division, Bedford, OH.
7. C.P. Germano, "Some Design Considerations in the Use of Bimorphs® as Motor Transducers" TP-237, Morgan Matroc Electro Ceramics Division, Bedford, OH.
8. G.H. Haertling, "Ultra-High-Displacement Actuator," *ACerS Bull* 73 [1], pp 93-96, 1994.

9. G.H. Haertling, "Cerambows: Pre-stressed Composite Ceramic Actuators," 1995 ONR Transducer Materials and Transducers Workshop, April 1995.
10. G.T. Stranford, personal communication, Aura Ceramics Inc., Minneapolis, MN.
11. J.P. Onders, "Investigation of Strain Transfer in a Smart Structure Adhesive Joint," M.S. Thesis, Mechanical Engineering, University of Toledo, Toledo, OH. 1993.
12. V. Giurgiutiu, Z.A. Chaudry, C.A. Rodgers, "Stiffness Issues in the Design of ISA Displacement Amplification Devices: Case Study of a Hydraulic Displacement Amplifier," *Smart Structures and Materials 1995*, Proc. SPIE 2443, 1995.
13. C.D. Near, et al, "Novel Methods of Powder Preparation and Ceramic Forming for Improving Reliability of Multilayer Ceramic Actuators," *Smart Structures and Materials 1993: Smart Materials*, Viray K. Varadan, Editor, Proc. SPIE 1916, pp 396-404, 1993.
14. C.D. Near and T.J. Meyer, "Testing Requirements and Performance Characterization of Multilayer Piezoelectric Actuators," in the Sixth US-Japan Seminar on Dielectric and Piezoelectric Ceramics, Program Summary and Abstracts, A. Safari, Editor, pp 352-355, 1993.
15. R.E. Newnham, Q.C. Xu, S. Yoshikawa, U.S. Patent No. 4,999,819.
16. Q.C. Xu, S. Yoshikawa, J.R. Belsick, and R.E. Newnham, "Piezoelectric Composites with High Sensitivity and High Capacitance for Use at High Pressures," *IEEE Trans. Ultrason., Ferroelectr., Freq. Control*, 38 [6], pp 634-639, 1991.
17. Y. Sugawara, K. Onitsuka, S. Yoshikawa, Q.C. Xu, R.E. Newnham, and K. Uchino, "Metal-Ceramic Composite Actuators," *J.Am.Cer.Soc.* 75 [4], pp 996-998, 1992.
18. A.L.W. Williams, et al., U.S. Patent No. 3,215,977.
19. T. Yano, I. Fukui, E. Sato, O. Inui, and Y. Miyazaki, "New Impact Printer Head Utilizing Stiffened Piezoelectric Effects," *Proc. IEEE Jpn.* 156, 1984.
20. M.G. Matsko, Q.C. Xu, and R.E. Newnham, "Zig-Zag Piezoelectric Actuators: Geometrical Control of Displacement and Resonance," unpublished.
21. W.P. Robbins, D. Polla, and D.E. Glumac, "High-Displacement Piezoelectric Actuator Utilizing a Meander-Line Geometry-Part I: Experimental Consideration," *IEEE Trans. Ultrason., Ferroelectr., Freq. Control*, 38 [5], pp 454-460, 1991.
22. W.P. Robbins, "High-Displacement Piezoelectric Actuator Utilizing a Meander-Line Geometry-Part II:," *IEEE Trans. Ultrason., Ferroelectr., Freq. Control*, 38 [5], pp 461-467, 1991.
23. U.S. Patent No. 4,995,587.
24. Q.M. Zhang, W.Y. Pan, S.J. Jang, and L.E. Cross, "Domain Wall Excitations and Their Contributions to the Weak-Signal Response of Doped Lead Zirconate Titanate Ceramics," *J. Appl. Phys.* 64 [11], pp 6445-6451, 1988.
25. D.A. Berlincourt and H.H.A. Krueger, "Behavior of Piezoelectric Ceramics Under Various Environmental and Operation Conditions of Radiating Sonar Transducers," TP-228, Morgan Matroc Electro Ceramics Division, Bedford, OH.